

Different optimization conditions required to enhance the reduction potential of silver nanoparticle biosynthesis via the Mycelia-free filtrate step using the fungus *Aspergillus flavus*

Khaled M Khleifat^{1,2*}, Haitham Qaralleh³, Mohammad A. Al-kafaween^{4*}, Muhamad O. Al-limoun², Moath Alqaraleh⁵, Abd Elalim Abu Sabha², Khalid A. Shadid⁵, Khalid Alqaisi¹, Rula Al Buqain⁶, Nida Karamah⁵, Hamid A. Nagi Al-Jama⁷, Malik Amonov⁸, Anas Abed⁵

¹ Department of Medical Laboratory Sciences, Faculty of Allied Medical Sciences, Al-Ahliyya Amman University, Amman, Jordan

² Department of Biological Sciences, Mutah University, Al-Karak, Jordan

³ Department of Medical Laboratory Analysis, College of Science, Mutah University, Al-Karak, Jordan

⁴ Faculty of Pharmacy, Department of Pharmacy, Al-Zaytoonah University of Jordan, Amman, Jordan

⁵ Pharmacological and Diagnostic Research Center (PDRC), Faculty of Pharmacy, Al-Ahliyya Amman University, Amman, Jordan

⁶ Cell Therapy Center- University of Jordan, Amman, Jordan

⁷ Faculty of Health Sciences, Universiti Sultan Zainal Abidin, Terengganu, Malaysia

⁸ Faculty of Medicine, Universiti Sultan Zainal Abidin, Terengganu, Malaysia

Abstract: **Introduction:** Fungi are one of the main approaches for synthesis of metallic nanoparticles (NPs), which can have medical and biotechnological applications such as their role in anti-bacterial, anti-cancer and various industrial activities. **Objective:** The current research focused on the biosynthesis of silver nanoparticles (AgNPs) using airborne fungi isolated from Al-karak general hospital operation rooms. **Materials and Methods:** The fungal isolate was identified at the species level by sequencing ITS as *Aspergillus flavus*. The confirmation and characterization of biosynthesized AgNPs were conducted using UV-Vis spectrophotometer, Zeta potential, Zeta sizer, FT-IR, XRD and transmission electron microscope (TEM) analyses. **Results:** The average diameter of the resulting AgNPs was 499.3 nm with a PDI value of 0.28. The zeta potential was -34.9mV which reflects the ability of these nanoparticles to have a sufficient charge, because it is electrostatically stable and therefore resists self-assembly. TEM revealed that these biosynthesized AgNPs were regular and spherical in shape. The images of TEM showed that the size of AgNPs were smaller than those that were observed by DLS examination due the drying process that caused particle shrinkage. The average size of AgNPs were less than 40 nm. AgNPs exhibit different minimal inhibitory concentrations (MIC) against seven different bacteria (*K. pneumoniae*, *E. coli*, *E. cloacae*, *S. aureus*, *S. epidermidis*, and *Shigella sp.*). The MICs ranged between 0.025 and 0.075 mg/mL with *P. aeruginosa* an exception which was the most resistant one, showing its MIC as > 0.125 mg/mL. **Discussion and Conclusion:** The results indicate that these molecules can be used as an important source for the treatment of many diseases caused by bacteria, in addition to testing these molecules in various fields such as cancer treatment and even in various biotechnological applications. **Keywords:** Nanoparticles, *Aspergillus flavus*, using UV-Vis spectrophotometer, Zeta potential, Zeta sizer

Correspondence to: Khaled M Khleifat, Department of Medical Laboratory Sciences, Faculty of Allied Medical Sciences, Al-Ahliyya Amman University, Amman, Jordan. Department of Biological Sciences, Mutah University, Al-Karak, Jordan; E-mail: alkh.kha@hotmail.com
Mohammad A. Al-kafaween, Faculty of Pharmacy, Department of Pharmacy, Al-Zaytoonah University of Jordan, Amman, Jordan; E-mail: mohammadalkafaween25@yahoo.com

Received: October 28, 2021; **Accepted:** November 28, 2021; **Published Online:** December 28, 2021

Citation: Khleifat, K.M., Qaralleh H., Al-kafaween, M.A., Al-limoun, M.O., Alqaraleh, M., Sabha, A.E.A., Shadid, K.A., Alqaisi, K., Buqain, R.A., Karamah, N., Al-Jama, H.A.N., Amonov, M., Abed, A., 2021. Different optimization conditions required to enhance the reduction potential of silver nanoparticle biosynthesis via the Mycelia-free filtrate step using the fungus *Aspergillus flavus*. *Applied Environmental Biotechnology*, 6(1): 42-50. <http://doi.org/10.26789/AEB.2021.01.005>

Copyright: Different optimization conditions required to enhance the reduction potential of silver nanoparticle biosynthesis via the Mycelia-free filtrate step using the fungus *Aspergillus flavus*. © 2021 Khaled M Khleifat et al. This is an Open Access article published by Urban Development Scientific Publishing Company. It is distributed under the terms of the [Creative Commons Attribution-Noncommercial 4.0 International License](https://creativecommons.org/licenses/by-nc/4.0/), permitting all non-commercial use, distribution, and reproduction in any medium, provided the original work is properly cited and acknowledged.

1 Introduction

Nanoscience is primarily concerned with the structure, physical, and chemical properties of nanoscale objects. On the other hand, nanotechnology is defined as the commercial, industrial, environmental, and medical applications of funda-

mental knowledge about nanoparticles (Satakar et al., 2016). Nanoscience and nanotechnology are both active branches of science that encompass a variety of interdisciplinary fields (Sergeev and Shabatina, 2008). All nanoscale objects, regardless of its nature, are referred to as nano-objects. The prefix 'nano' refers to a millionth of a millimeter in size. The

term “objects” can be modified with any other phrase that accurately describes the nature of these objects (Ingole et al., 2010), which may be particles, fibers, or plates (Calderón-Jiménez et al., 2017). The findings of basic knowledge about nanoscale objects have distinctively altered the industrial world’s standpoint, with nanoscale construction blocks and materials now being used globally (Ingole et al., 2010). They have unique and different size-related physico-chemical properties (Colvin et al., 1994; Xu et al., 2006). Metal nanoparticles have unique physical and chemical properties due to their nano size and high surface area (Gentile et al., 2016).

Silver containing products are widely used for their antibacterial properties in a variety of medical applications including burns and infections. The antibacterial effects of silver ions are very well established. Nonetheless, the design of a process for silver colloid particles synthesis in which size and morphology are controlled has attracted a great attention in the nano-biotechnology field (Al-Bakri and Mahmoud, 2019; Qaralleh et al., 2019). Silver nanoparticles were commonly formed using three major methods: chemical, physical, and biological. As an environmentally friendly, cost-effective, and safe method of synthesis without the use of toxic chemicals and without the formation of hazardous byproducts, several extracellular and intracellular biological methods utilizing bacteria, fungi, plants, or their extracts have been reported, collectively referred to as green nanotechnology (Klaus et al., 1999). The *fungal species* used in this study was isolated from the Al-karak general hospital operation rooms. It was identified as *Aspergillus flavus* (MACROGEN, Korea) using internal transcribed spacer (ITS) sequencing. The present study objectives were to optimize the conditions of AgNO₃ containing fungal biomass free solution employed in AgNPs synthesis using *Aspergillus flavus*, to characterize the synthesized AgNPs using UV-visible spectrophotometer, TEM, ATR-IR, XRD and Z-potential and evaluate the antibacterial activity of AgNPs against Gram-positive and Gram-negative bacteria.

2 Materials and Methods

2.1 Fungal strain

Aspergillus flavus used in this study was provided by Dr. Amjad Al-Tarawneh (the Dead Sea Center for Water and Energy at Mutah University, Jordan). This species was isolated from the warehouses of the Supplies Department at Mutah University. It was identified as *Aspergillus flavus* (MACROGEN, Korea) using ITS sequencing. The sequence was registered at the NCBI database and the accession number MG973280.1 was obtained.

2.2 Preparation of culture conditions for *Aspergillus flavus*

Aspergillus flavus spores adjusted to 2.0×10^6 was grown in a complex broth media containing 10 g glucose, 10 g yeast

extract and 5 g NaCl (pH 7). The culture was incubated at 33°C, 150 rpm for 72h. The culture was then filtrated using filter paper Whatmann No. 1 and the mycelia (biomass) was collected and washed thoroughly with deionized distilled water. Subsequently, the freshly prepared biomass was used for the next step (preparation of biomass filtrate) (Bader et al., 2007).

2.3 Biosynthesis of AgNPs

The synthesis of silver nanoparticles (AgNPs) was performed according to (Jaidev and Narasimha, 2010) with some modifications. Briefly, 10 g of previously described crude biomass was soaked in 100 mL sterile deionized water at 33°C, pH 7.0 and 150 rpm. at the designated timepoint, the crude biomass was removed by filtration (Whatmann No.1) and the suspension (biomass free fungal filtrate) was collected. The collected biomass free fungal filtrate was used for AgNPs synthesis. This was performed by mixing 100 mL of the filtrate with different concentrations of silver nitrate (AgNO₃). The mixture was then incubated at 27°C, 150 rpm for 72h in the dark.

2.4 Optimization of AgNPs biosynthesis parameters

Multiple parameters were investigated in this study to optimize the conditions for AgNPs synthesis. The parameters tested in this study were in the following order: temperature, pH, the concentrations of AgNO₃ and the incubation period. 100 mL of biomass free fungal filtrate was mixed with different concentrations of AgNO₃ (0.5, 1.0, 1.5 and 2.0 mM) and incubated at different temperatures (25, 27 and 30°C), different pH (4, 5, 6, 7, 8 and 9) and different incubation periods (0, 24, 48, 72, 96, 120, 144 and 168h). For all tested parameters, UV-visible scanning spectroscopy was used to evaluate the synthesized nanoparticles.

2.5 Characterization of AgNPs

The synthesized AgNPs were initially characterized using a spectrophotometer (UV-1800 spectrophotometer (SHIMADZU, Japan)). The samples were monitored at ultraviolet-visible (UV/VIS) light ranged from 280 to 800 nm. The synthesized AgNPs were concentrated by centrifugation at 15000 rpm for 20 min. This step was repeated several times. The collected pellet was then dried using a vacuum dryer (VWR 1410 Vacuum Oven, USA). TEM images of the synthesized AgNPs were taken by an FEI Versa 3D Dual Beam instrument (FEI, USA) and the AgNPs crystals were detected using MAXima-X XRD-7000 (SHIMADZU, Japan). The ATR-IR for the synthesized AgNPs was analyzed using a Bruker Alpha FTIR spectrometer (Bruker Optics GmbH, Ettlingen, Germany). The diameter, polydispersity index (PDI), and the zeta potential of AgNPs were measured using Zetasizer Nano-ZS90 (Malvern Instruments, UK). Different

concentrations of AgNPs were analyzed at a 90-degree scattering angle at a temperature of 25°C.

2.6 Antibacterial activity of AgNPs

AgNPs stock solutions of 25 mg/mL was used to prepare various concentrations of AgNPs in Muller Hinton broth (0.025-1.5 mg/ml) which was then added to a 96-well plate (Al-kafaween et al., 2021; Al-kafaween et al., 2020; Tarawneh et al., 2021). 10 L of the different bacterial strains' suspension equivalent to 0.5 McFarland standards (approximately 108 CFU/mL for bacteria) was added to each well. Three different antibiotics including chloramphenicol (Cm), kanamycin (Km) and ampicillin (Amp) were used as positive controls. The inoculated plates were incubated at 37°C for 24h. The growth of the bacteria was monitored by the subculture of each well content on nutrient agar (Al-Asoufi et al., 2017; Al-kafaween and Hilmi, 2022; et al., ; Khleifat et al., 2006; Khleifat et al., 2006; Khleifat et al., 2010; Khleifat et al., 2008; Tarawneh et al., 2009; Tarawneh et al., 2021; Yousef et al., 2021). The minimum inhibitory concentration (MIC) values were defined as the lowest concentrations of the AgNPs found to inhibit the growth of bacteria (Al-kafaween et al., 2021; Al-kafaween et al., 2021).

3 Results and Discussion

The employment of fungi extracts as reductants and stabilizers in the synthesis of AgNPs is interesting due to the high yield, ease of processing, and low cytotoxicity of the residues. Furthermore, this biosynthesis process may result in enhanced stability and even improved biological activity due to the presence of fungi-derived biomolecules at the surface of particles (Durán et al., 2016; Guilger-Casagrande and Lima, 2019; Rahimi et al., 2016). Fungi are used to synthesize silver nanoparticles by first cultivating them in liquid medium. Following biomass production, the biomass is soaked in water for the extraction of the metabolites involved in the synthesis. After filtration, the biomass is removed and the filtrate is treated with silver nitrate (Jarrar et al., 2020; Ottoni et al., 2017). Consequently, the color of the mixture changes following the reaction, and UV-visible spectroscopy can be used to observe SPR peaks reflecting changes in the material's optical properties (Ahmad et al., 2003). These bands have absorbance wavelengths ranging from 400 to 450 nm, with a greater wavelength suggesting the presence of bigger nanoparticles (Elamawi et al., 2018). The size of the nanoparticles is dependent on the fungus species, incubation temperature, pH of the mixture, and the occurrence of nanoparticle cappings (Khandel and Shahi, 2018; Lee and Jun, 2019). The mixture is also influenced by the SPR, which changes depending on the size and absorbance of the nanoparticles (Lee and Jun, 2019).

Due to the diversity of fungi that may be used in AgNPs synthesis, it is critical to optimize the synthesis parameters

appropriately. In this study, the aqueous extracts of fungus *Aspergillus flavus* filtrate was used to synthesize AgNPs. The possibility to use *A. flavus* filtrate to carry out the AgNPs synthesis under a variety of conditions, including incubation temperature and period, pH, crude concentration, and AgNO₃ concentration, allows the generation of nanoparticles with a variety of physicochemical properties (Guilger-Casagrande and Lima, 2019).

3.1 UV-vis absorption spectra (UV-vis)

The formation of AgNPs was initially indicated by visual observation (Figure 1). During the synthesis process the colorless AgNO₃ turned to dark brown color after 72h. Furthermore, the formation of AgNPs was confirmed using UV-vis spectroscopy and the surface plasmon resonance (SPR) analyses. These analyses were performed based on fact that the reduction of AgNO₃ ions to silver atoms (Ag⁰) results in the absorption of UV radiation at a wavelength range of 400-500 nm that eventually ends up with color change. As shown in Figure 1, the SPR peak was observed at 479 nm. In fact, the size, shape and number of the formed nanoparticles are reflected in the intensity of the absorption peak (Jaidev and Narasimha, 2010; Riaz et al., 2021). The formation of AgNPs appears to occur by one of two possible mechanisms, either by NADH-dependent nitrate reductase or by the shuttle quinone process (Basavaraja et al., 2008; Durán et al., 2005; Jaidev and Narasimha, 2010; Kalimuthu et al., 2008). The results of the present study indicate that the formation of nanoparticles occurs in the extracellular media due to the action of extracellular nitrate reductase.

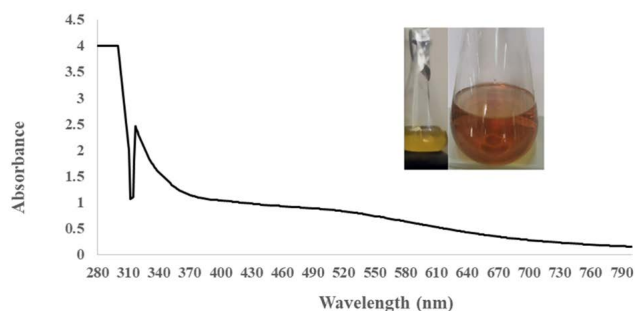


Figure 1. Biosynthesis of AgNPs using 1 mM AgNO₃ and fungal biomass free filtrate prior to optimization process. The growth conditions were 33°C, pH 7 and 10 g for incubation temperature, pH and fungal biomass, respectively. (a) color change and (b) Ultraviolet-Visible spectra

3.2 Effects of incubation temperature on AgNPs synthesis by biomass-free filtrate

The effect of incubation temperature on the synthesis of AgNPs was evaluated at 25, 27 and 30°C with a constant agitation rate at 150 rpm for 72h. The results (Figure 2) showed that the maximum rate of AgNPs synthesis (indicated by the

intensity of the absorption) was optimally obtained at incubation temperature of 27°C. Generally speaking, the SPR was as a shoulder-like peak. However, altering the incubation temperature led to variation in the extent of shoulder-like peaks represented as 400 nm, 380 nm and 510 nm for incubation temperatures of 27, 30 and 25°C, respectively. An important factor influencing the effect of temperature on the formation of nanoparticles is the enzymes that could be part of the collected fungi filtrate (Garg, 2015). The results presented here suggested that as the incubation temperature increased from 25 to 27°C, the activity of the AgNPs dependent enzymes increased thus, the formation of AgNPs was increased (Gurunathan et al., 2009). On the contrary, further increase in incubation temperature to 30°C led to lowering number of nanoparticles. Additionally, the presence of a shoulder-like peak may confirm the presence of a variety of biological molecules, as indicated by the width and shape of the SPR band (Huang et al., 2011). For instance, when the monocular SPR is narrow, it indicates the presence of a single diffuse of spherical particles, whereas the wide band indicates the presence of a diverse distribution of particles of various sizes (Riaz et al., 2021).

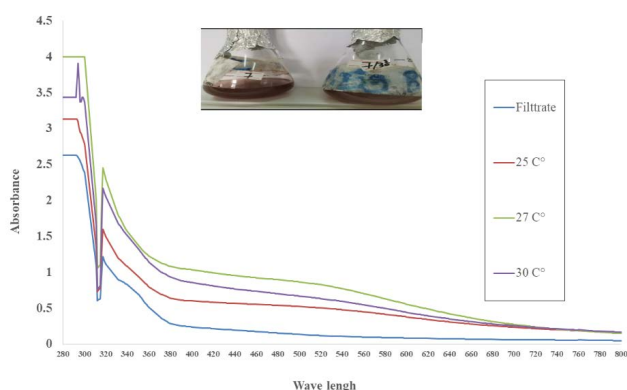


Figure 2. Effect of incubation temperature on AgNPs synthesis by biomass-free filtrate of *Aspergillus flavus*

3.3 Effect of pH on AgNPs synthesis by biomass-free filtrate

In order to evaluate the effect of various pH values on the formation of AgNPs, pHs of 4, 5, 6, 7, 8 and 9. These pH values were selected to represent the acidic, neutral, and alkaline conditions. The rate of AgNPs synthesis, shape and size of AgNPs are pH dependent (Guilger-Casagrande and Lima, 2019). Figure 3 demonstrates the effect of different pH values on AgNPs formation. The rate of AgNPs synthesis was maximum at pH 7 which was indicated by absorbance (OD) values. In contrast, the rate of synthesis tends to decrease when the pH value rises (8 and 9) and reach the lowest at acidic pHs (4, 5 and 6). Additionally, the SPR peaks for the synthesized AgNPs under acidic conditions (pH 4, 5 and 6) appear early at shorter wavelengths (< 400 nm), whereas,

when AgNPs biosynthesized at pH 7 or above, the SPR peaks appeared at 410 nm. Thus, the formation of AgNPs in terms of rate of synthesis and morphology was optimum at a pH of 7. In acidic conditions, the nucleation process for the formation of AgNPs occurs at a very slow rate. As the pH increases, the rate of nucleation process increases because of the accessibility of -OH ions. Thus, nanoparticle intensity increases, and size becomes smaller (Chitra and Annadurai, 2014).

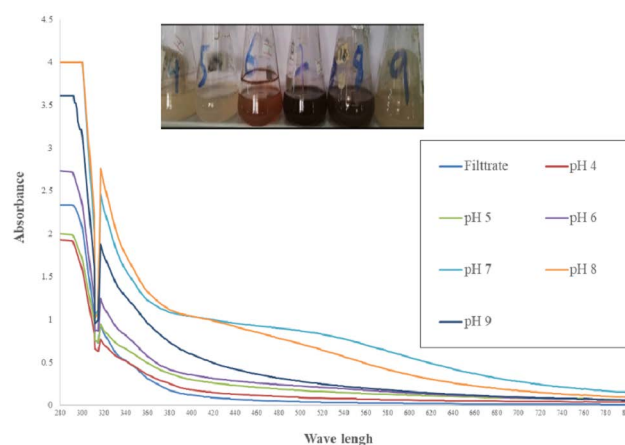


Figure 3. Effect of pH on AgNPs synthesis by biomass-free filtrate of *Aspergillus flavus*

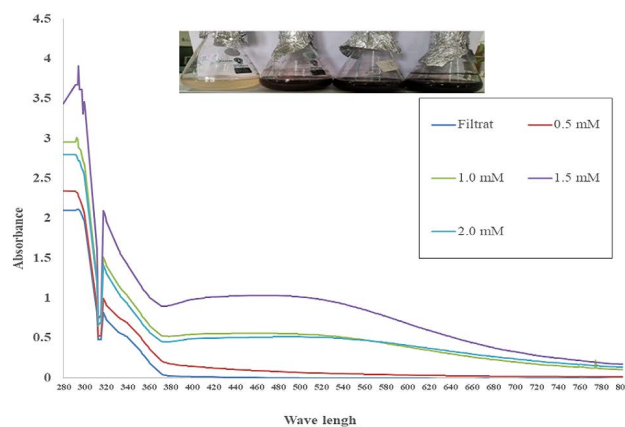


Figure 4. Effect of AgNO₃ concentration on AgNPs synthesis by biomass-free filtrate of *Aspergillus flavus*

3.4 Effect of AgNO₃ concentration on AgNPs synthesis by biomass-free filtrate

In order to evaluate the effect of the concentration of AgNO₃ on the formation of AgNPs, different concentrations of silver nitrate salt (0.5, 1.0, 1.5 and 2.0 mM) were used. As shown in Figure 4, the maximum rate of AgNPs synthesis was observed at a concentration of 1.5 mM AgNO₃. In contrast, the rate of synthesis was lower at concentrations equal to 2 and 1.0 mM, whereas the lowest rate was observed at a concentration of 0.5 mM AgNO₃. Thus, the synthesis of nanoparticles

is not AgNO_3 concentration dependent. Instead, it obeys the saturation nature of the enzymes (Singh et al., 2013).

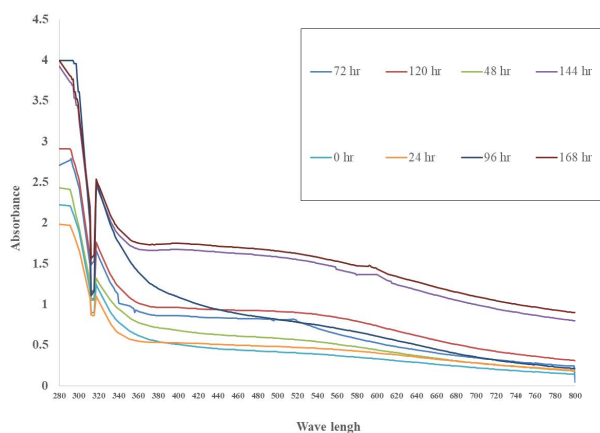


Figure 5. Effect of incubation time on AgNPs synthesis by biomass-free filtrate of *Aspergillus flavus*

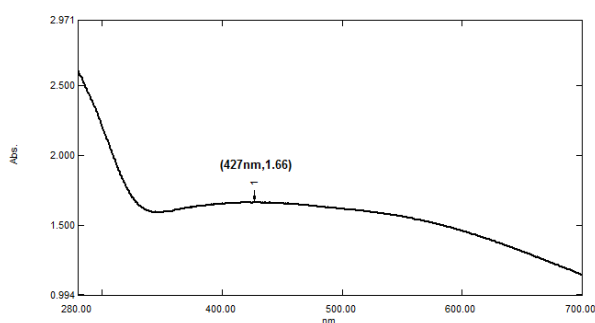


Figure 6. Solution of 1.5 mM AgNO_3 after bioreduction by biomass free filtrate of *Aspergillus flavus* following optimization process. Incubation temperature was at 27°C using 10 g biomass, and pH of 7

3.5 Effect of incubation time on AgNPs synthesis by biomass-free filtrate

To identify the best incubation time for maximum nanoparticle synthesis, AgNO_3 was added to biomass free filtrate and incubated at 27°C and pH of 7.0 for different intervals (24, 48, 72, 96, 120, 144 and 168 hours) (Figure 5). At the designated timepoint, a sample was taken and the formation of AgNPs was determined for each sample using UV-vis spectroscopy. Unsurprisingly, there was no evidence of nanoparticle formation at zero hour. However, as the incubation time increase, the rate of nanoparticle formation increased and reached the maximum after 144 and 168 hours. Interestingly, there was no dramatic change in the rate of AgNPs synthesis between 144 and 168 hours timepoint indicating that the 144 h period of incubation was optimal and full reduction of Ag ions. After the reaction conditions were optimized, the stability of silver nanoparticle solution was assessed using UV-vis spectroscopy. The nanoparticle

solution showed a remarkable stability for more than three months, with no evidence of aggregation as noted by FTIR findings (see below). This stability is potentially attributed to the capping of the synthesized particles by the proteins secreted by the biomass into the filtrate (Sastry et al., 2003). The optimized crude sample exhibited an interesting UV-vis spectral peak at 479 nanometers (Figure 1), whereas after extensive purification with deionized distilled water, the optimized sample exhibited a peak at 427 nanometers (Figure 6).

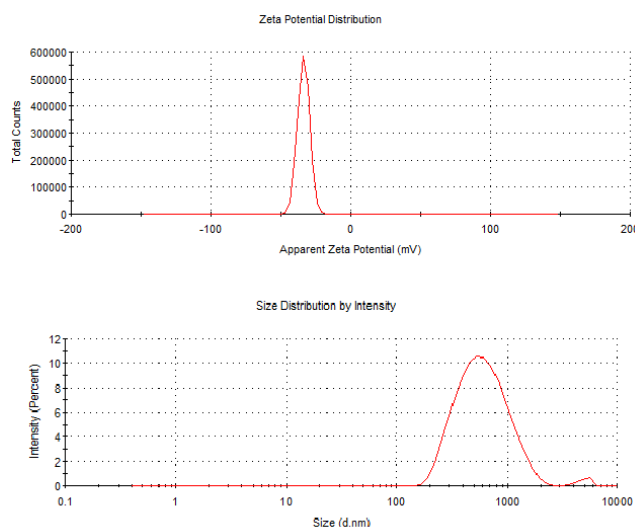


Figure 7. Zeta potential and size distribution of silver nanoparticles

3.6 Characterization of biosynthesized AgNPs

Following synthesis, the resulted AgNPs were characterized using in terms of size, PDI, and zeta potential using zetasizer (Figure 7). The analysis revealed that AgNPs had an average size of 499.3 nm, a PDI of 0.28 indicating a polydispersed formulation and a zeta potential of -34.9mV indicating electrostatic stability. The size and the morphology of AgNPs were further assessed by Transmission electron microscope (TEM) which revealed a regular and spherical shape of the formed particles (Figure 8 and Figure 9). Interestingly, TEM micrographs demonstrated that the average size of AgNPs was substantially smaller than those observed by DLS examination (< 40 nm). This could be attributed to the drying process coincided with sample preparation for TEM imaging which may have resulted in particle shrinkage.

TEM (Figure 7). The TEM image revealed that the formed nanoparticles were spherical in shape and the diameter of the nanoparticles was between 10 to 35 nm.

3.7 FTIR spectrum analysis

The furrier transformed infrared (FTIR) spectroscopy analysis was carried out to purposely identify the biomolecules and

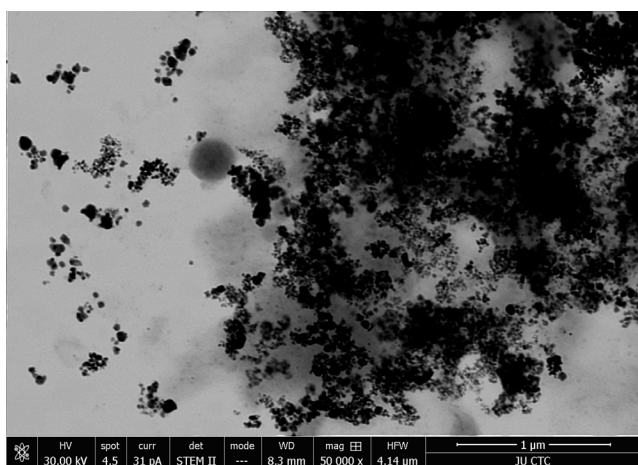


Figure 8. Image of biosynthesized silver nanoparticles. Scale bar = 1μm

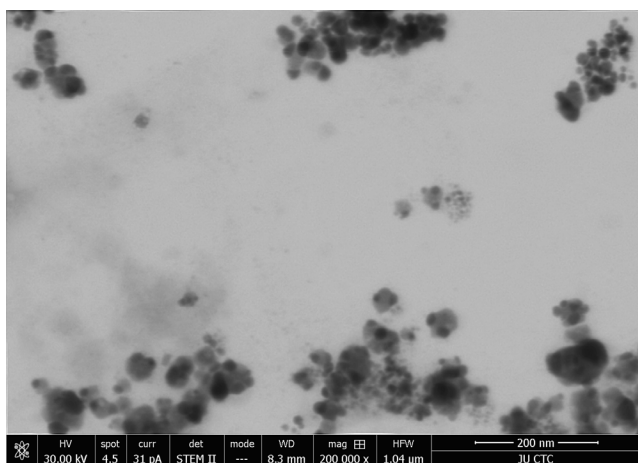


Figure 9. Image of biosynthesized silver nanoparticles. Scale bar = 200 nm

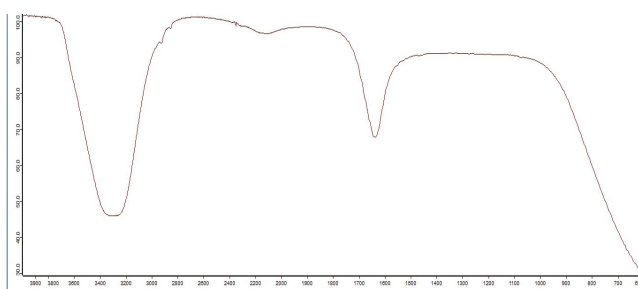


Figure 10. FTIR spectrum of biologically synthesized of silver nanoparticles

functional groups that might be responsible of the reduction of silver nitrate ions as well as the capping of the bio-reduced synthesized AgNPs. The FTIR absorption spectrum (Figure 10) showed a characteristic absorption band at 3400 cm^{-1} indicating the presence of OH group of water molecules. Absorption bands at 2918 and 2850 cm^{-1} suggested the presence of C-H bond while the absorption band at 1650 cm^{-1} suggested the presence of C-N and C-C bonds and the band at 1450 suggested the presence of N-H and C-N bonds.

3.8 Powder X-ray diffraction (XRD) analysis

The crystallographic structure of the formed AgNPs was determined using XRD with diffracted scans recorded from $2\theta = 5^\circ$ to 65° . As shown in (Figure 11), the AgNPs exhibited a number of Bragg's reflections at 27.77° , 32.18° , 38.10° , 46.17° , 54.74° , and 57.69° . Among these, the reflection at 38.10 corresponds to (1 1 1) planes of crystalline silver metal particles suggesting that the AgNPs formed were of premium quality and that the synthesized AgNPs had a face-centered cubic shape. Thus, the XRD analysis revealed a high purity and multicrystalline nature of the synthesized particles.

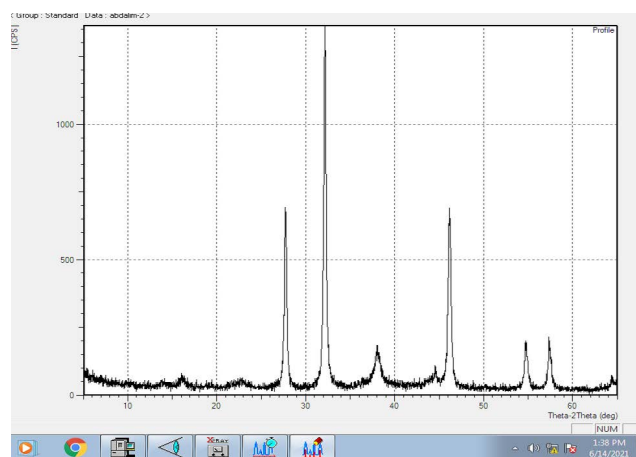


Figure 11. XRD Analysis of biological synthesis of Silver Nanoparticles

3.9 Antibacterial activity of AgNPs

Following synthesis and characterization, the antibacterial effect of the synthesized AgNPs colloid was investigated on multiple bacterial strains. MIC is the minimum inhibitory concentration required to inhibit the growth of the microorganism where low MIC value reflects a potent antimicrobial property. As shown in (Table 1), the lowest MIC indicated was against *K. pneumonia* and *E. cloacae* (0.025 mg/mL) followed by *S. epidermidis* (0.05 mg/mL), *E. coli* (0.075 mg/mL), *Shigella sp.* (mg/mL) and *S. aureus* (0.10 mg/mL). on the contrary, the *P. aeruginosa* showed a lower susceptibility indicated by MIC value of $> 0.125\text{ mg/ml}$ of AgNPs. Based on the previous results, it can be said that AgNPs possess broad spectrum antibacterial activity. The inhibition

of gram positive and gram negative bacterial species at low concentrations ranging from 0.025 - 0.10 mg/mL indicated the remarkable antibacterial activity of AgNPs. AgNPs have long been recognized for their broad-spectrum antimicrobial activity (Bocate et al., 2019; Haggag et al., 2019; Qaralleh et al., 2019). In this study, AgNPs exhibited broad spectrum antibacterial activity against both gram positive and gram negative bacteria. Our findings are consistent with those of (Arokiyaraj et al., 2017; Qaralleh et al., 2019). NPs interfere with the integrity of the bacterial cell wall, which in turn expedites permeation of substances into and out of the bacterial cell. This mechanism of AgNPs action might also encompass the creation of reactive oxygen species (ROS), which in turn can cause higher toxicity and through the inhibition of the respiratory chain of bacteria (Al-limoun et al., 2020; Sondi and Salopek-Sondi, 2004).

Table 1. The minimum inhibitory concentrations (MIC) for each organism were determined while the concentration is provided in g/mL

Amp	Km	Cm	AgNPs	Bacteria
3	0.15	0.75	75	<i>E. coli</i>
2	0.1	0.1	25	<i>E. cloacae</i>
3	0.15	0.1	75	<i>Shigella sp.</i>
5	0.25	1	>125	<i>P. aeruginosa</i>
0.25	0.3	0.1	50	<i>S. epidermidis</i>
0.5	10	0.25	100	<i>S. aureus</i>
5	0.5	0.1	50	<i>K. pneumoniae</i>

4 Discussion

All in all, the results presented in this study showed that the biomass-free filtrate obtained from the fungal isolate *Aspergillus flavus*, was able to reduce silver nitrate into AgNPs. The production of AgNPs was confirmed and characterized through using various methods including the change in the silver nitrate solution color, UV-vis spectra, TEM, Zeta potential, Zeta sizer, FTIR, and XRD. TEM revealed that these biosynthesized AgNPs were regular and spherical in shape. Intriguingly, the images of TEM showed that the size of AgNPs were smaller than those obtained by DLS examination due the drying process that caused particle shrinkage. The average diameter of the resulting AgNPs was 499.3 nm with a PDI value of 0.28. The zeta potential was -34.9mV which reflects the ability of these nanoparticles to have a sufficient charge, because it is electrostatically stable and therefore resists self-assembly. The average size of AgNPs were less than 40 nm. AgNPs exhibit different minimal inhibitory concentrations (MIC) against seven different bacteria. Thus, the use of silver nanoparticles to inhibit the growth of these antibiotic-resistant or even still antibiotic-sensitive bacteria is an important result and an effective master treatment plan.

Funding Sources

This work was supported by Universiti Sultan Zainal Abidin (UniSZA) and Deanship of scientific research at Mutah University, Jordan.

Acknowledgments

We thank all the staff members of the Faculty of Health Sciences and Faculty of Sciences at Universiti Sultan Zainal Abidin and Mu'tah University for their support and commitment.

Conflict of Interest

The authors declare that there is no conflict of interest regarding the publication of this article.

Author Contributions

All authors made substantial contributions to conception and design, acquisition of data, or analysis and interpretation of data.

References

- Ahmad, A., Mukherjee, P., Senapati, S., Mandal, D., Khan, M.I., Kumar, R., Sastry, M., 2003. Extracellular biosynthesis of silver nanoparticles using the fungus *Fusarium oxysporum*. *Colloids and Surfaces B: Biointerfaces*, 28(4): 313-318.
[https://doi.org/10.1016/S0927-7765\(02\)00174-1](https://doi.org/10.1016/S0927-7765(02)00174-1)
- Al-Asoufi, A., Khlaifat, A., Tarawneh, A., Alsharafa, K., Al-Limoun, M., Khleifat, K., 2017. Bacterial Quality of Urinary Tract Infections in Diabetic and Non Diabetics of the Population of Ma'an Province, Jordan. *Pakistan Journal of Biological Sciences*, 20(4): 179-188.
<https://doi.org/10.3923/pjbs.2017.179.188>
- Al-Bakri, A.G. and Mahmoud, N.N., 2019. Photothermal-induced antibacterial activity of gold nanorods loaded into polymeric hydrogel against *Pseudomonas aeruginosa* biofilm. *Molecules*, 24(14): 2661.
<https://doi.org/10.3390/molecules24142661>
- Al-kafaween, M.A., Hilmi, A.B.M., Al-Jamal, H.A.N., Al-Groom, R.M., Elshahry, N.A., Al-Sayyed, H., 2021. Potential Antibacterial Activity of Yemeni Sidr Honey Against *Pseudomonas aeruginosa* and *Streptococcus pyogenes*. *Anti-Infective Agents*, 19(4): 51-65.
<https://doi.org/10.2174/2211352519666210319100204>
- Al-kafaween, M.A., Hilmi, A.B.M., Al-Jamal, H.A.N., Elshahry, N.A., Jaffar, N., Zahri, M.K., 2020. *Pseudomonas Aeruginosa* and *Streptococcus Pyogenes* Exposed to Malaysian Trigona Honey In Vitro Demonstrated Downregulation of Virulence Factor. *Iranian Journal of Biotechnology*, 18(4): 115-123.
- Al-kafaween, M.A., Hilmi, A.B.M., Jaffar, N., Al-Jamal, H.A.N., Zahri, M.K., Jibril, F.I., 2020. Antibacterial and Antibiofilm activities of Malaysian Trigona honey against *Pseudomonas aeruginosa* ATCC 10145 and *Streptococcus pyogenes* ATCC 19615. *Jordan Journal of Biological Sciences*, 13(1): 69 - 76.
- Al-kafaween, M.A. and Hilmi, A.B.M., 2022. Evaluation of the effect of different growth media and incubation time on the suitability of biofilm formation by *Pseudomonas aeruginosa* and *Streptococcus pyogenes*. *Applied Environmental Biotechnology*, 6(2): 19-26.
<https://doi.org/10.26789/AEB.2021.02.003>

- Al-kafaween M.A., Abu Bakar M.H., Al-Jamal, H.A.N., 2021. The Beneficial Effects of Stingless Bee Kelulut Honey Against *Pseudomonas aeruginosa* and *Streptococcus pyogenes* Planktonic and Biofilm. *Tropical Journal of Natural Product Research*, 5(10): 1788-1796. <https://doi.org/10.26538/tjnpr/v5i10.15>
- Al-kafaween M.A., Al-Jamal, H.A.N., Hilmi, A.B.M., Elshoryi, N.A., Jaffar, N., Khairi Z., 2020. Antibacterial properties of selected Malaysian Tualang honey against *Pseudomonas aeruginosa* and *Streptococcus pyogenes*. *Iranian Journal of Microbiology*, 12(6): 565-576.
- Al-limoun, M., Qaralleh, H.N., Khleifat, K.M., Al-Anber, M., Al-Tarawneh, A., Al-sharafa, K., Al-soub, T., 2020. Culture Media Composition and Reduction Potential Optimization of Mycelia-free Filtrate for the Biosynthesis of Silver Nanoparticles Using the Fungus *Trichium oryzae* W5H. *Current Nanoscience*, 16(5): 757-769. <https://doi.org/10.2174/1573413715666190725111956>
- Althunibat, O.Y., Qaralleh, H., Al-Dalin, S.Y. A., Abboud, M., Khleifat, K., Majali, I.S., Jaafra, A., 2016. Effect of thymol and carvacrol, the major components of Thymus capitatus on the growth of *Pseudomonas aeruginosa*. *Journal of Applied Microbiology*, 10(1): 367-374.
- Arokiyaraj, S., Vincent, S., Saravanan, M., Lee, Y., Oh, Y.K., Kim, K.H., 2017. Green synthesis of silver nanoparticles using *Rheum palmatum* root extract and their antibacterial activity against *Staphylococcus aureus* and *Pseudomonas aeruginosa*. *Artificial Cells, Nanomedicine & Biotechnology*, 45(2): 372-379. <https://doi.org/10.3109/21691401.2016.1160403>
- Bader, A., Panizzi, L., Cioni, P.L., Flamini, G., 2007. *Achillea ligustica*: composition and antimicrobial activity of essential oils from the leaves, flowers and some pure constituents. *Central European Journal of Biology*, 2(2): 206-212. <https://doi.org/10.2478/s11535-007-0020-3>
- Basavaraja, S., Balaji, S., Lagashetty, A., Rajasab, A., Venkataraman, A., 2008. Extracellular biosynthesis of silver nanoparticles using the fungus *Fusarium semitectum*. *Materials Research Bulletin*, 43(5): 1164-1170. <https://doi.org/10.1016/j.materresbull.2007.06.020>
- Bocate, K.P., Reis, G.F., de Souza, P.C., Junior, A.G.O., Durn, N., Nakazato, G., Panagio, L.A., 2019. Antifungal activity of silver nanoparticles and simvastatin against toxigenic species of *Aspergillus*. *International Journal of Food Microbiology*, 291, 79-86. <https://doi.org/10.1016/j.ijfoodmicro.2018.11.012>
- Calderón-Jiménez, B., Johnson, M.E., Montoro Bustos, A.R., Murphy, K.E., Winchester, M.R., Vega Baudrit, J.R., 2017. Silver nanoparticles: technological advances, societal impacts, and metrological challenges. *Frontiers in Chemistry*, 5, 6. <https://doi.org/10.3389/fchem.2017.00006>
- Chitra, K., and Annadurai, G., 2014. Antibacterial activity of pH-dependent biosynthesized silver nanoparticles against clinical pathogen. *BioMed Research International*, 2014. <https://doi.org/10.1155/2014/725165>
- Colvin, V.L., Schlamp, M.C., Alivisatos, A.P., 1994. Light-emitting diodes made from cadmium selenide nanocrystals and a semiconducting polymer. *Nature*, 370(6488): 354-357. <https://doi.org/10.1038/370354a0>
- Durán, N., Durn, M., De Jesus, M.B., Seabra, A.B., Fvaro, W.J., Nakazato, G., 2016. Silver nanoparticles: A new view on mechanistic aspects on antimicrobial activity. *Nanomedicine: Nanotechnology, Biology and Medicine*, 12(3): 789-799. <https://doi.org/10.1016/j.nano.2015.11.016>
- Durán, N., Marcato, P.D., Alves, O.L., De Souza, G.I., Esposito, E., 2005. Mechanistic aspects of biosynthesis of silver nanoparticles by several *Fusarium oxysporum* strains. *Journal of Nanobiotechnology*, 3(1): 1-7. <https://doi.org/10.1186/1477-3155-3-8>
- Elamawi, R.M., Al-Harbi, R.E., Hendi, A.A., 2018. Biosynthesis and characterization of silver nanoparticles using *Trichoderma longibrachiatum* and their effect on phytopathogenic fungi. *Egyptian Journal of Biological Pest Control*, 28(1): 1-11. <https://doi.org/10.1186/s41938-018-0028-1>
- Garg, H., 2015. An approach for solving constrained reliability-redundancy allocation problems using cuckoo search algorithm. *Beni-Suef University Journal of Basic and Applied Sciences*, 4(1): 14-25. <https://doi.org/10.1016/j.bjbas.2015.02.003>
- Gentile, A., Ruffino, F., Grimaldi, M. G., 2016. Complex-morphology metal-based nanostructures: Fabrication, characterization, and applications. *Nanomaterials*, 6(6): 110. <https://doi.org/10.3390/nano6060110>
- Guilger-Casagrande, M. and Lima, R.D., 2019. Synthesis of silver nanoparticles mediated by fungi: a review. *Frontiers in Bioengineering and Biotechnology*, 7, 287. <https://doi.org/10.3389/fbioe.2019.00287>
- Gurunathan, S., Kalishwaralal, K., Vaidyanathan, R., Venkataraman, D., Pandian, S.R.K., Muniyandi, J., Eom, S.H., 2009. Biosynthesis, purification and characterization of silver nanoparticles using *Escherichia coli*. *Colloids and surfaces B: Biointerfaces*, 74(1): 328-335. <https://doi.org/10.1016/j.colsurfb.2009.07.048>
- Haggag, E.G., Elshamy, A.M., Rabeh, M.A., Gabr, N.M., Salem, M., Youssif, K.A., Abdelmohsen, U.R., 2019. Antiviral potential of green synthesized silver nanoparticles of *Lampranthus coccineus* and *Malephora lutea*. *International Journal of Nanomedicine*, 14, 6217. <https://doi.org/10.2147/IJN.S214171>
- Huang, J., Zhan, G., Zheng, B., Sun, D., Lu, F., Lin, Y., Li, Q., 2011. Biogenic silver nanoparticles by *Cacumen platycladi* extract: synthesis, formation mechanism, and antibacterial activity. *Industrial & Engineering Chemistry Research*, 50(15): 9095-9106. <https://doi.org/10.1021/ie200858y>
- Ingole, A.R., Thakare, S.R., Khati, N., Wankhade, A.V., Burghate, D., 2010. Green synthesis of selenium nanoparticles under ambient condition. *Chalcogenide Lett*, 7(7): 485-489.
- Jaidev, L. and Narasimha, G., 2010. Fungal mediated biosynthesis of silver nanoparticles, characterization and antimicrobial activity. *Colloids and Surfaces B: Biointerfaces*, 81(2): 430-433. <https://doi.org/10.1016/j.colsurfb.2010.07.033>
- Jarrar, Y., Al-Doaiss, A., Alfaihi, M., Shati, A., Al-Kahtani, M., Jarrar, B., 2020. The influence of five metallic nanoparticles on the expression of major drug-metabolizing enzyme genes with correlation of inflammation in mouse livers. *Environmental Toxicology and Pharmacology*, 80, 1034-1049. <https://doi.org/10.1016/j.etap.2020.103449>
- Kalimuthu, K., Babu, R.S., Venkataraman, D., Bilal, M., Gurunathan, S., 2008. Biosynthesis of silver nanocrystals by *Bacillus licheniformis*. *Colloids and Surfaces B: Biointerfaces*, 65(1): 150-153. <https://doi.org/10.1016/j.colsurfb.2008.02.018>
- Khandel, P. and Shahi, S.K., 2018. Mycogenic nanoparticles and their bio-prospective applications: current status and future challenges. *Journal of Nanostructure in Chemistry*, 8(4): 369-391. <https://doi.org/10.1007/s40097-018-0285-2>
- Khleifat, K., Abboud, M., Al-Shamayleh, W., Jiries, A., Tarawneh, K., 2006. Effect of chlorination treatment on gram negative bacterial composition of recycled wastewater. *Pakistan Journal of Biological Sciences*, 9, 1660-1668. <https://doi.org/10.3923/pjbs.2006.1660.1668>
- Khleifat, K.M., Abboud, M.M., Al-Mustafa, A.H., Al-Sharafa, K.Y., 2006. Effects of carbon source and *Vitreoscilla hemoglobin* (VHb) on the production of -galactosidase in *Enterobacter aerogenes*. *Current Microbiology*, 53(4): 277-281. <https://doi.org/10.1007/s00284-005-0466-3>
- Khleifat, K.M., Halasah, R.A., Tarawneh, K.A., Halasah, Z., Shawabkeh, R., Wedyan, M.A., 2010. Biodegradation of linear alkylbenzene sulfonate by *Burkholderia* sp.: Effect of some growth conditions. *International Journal of Agricultural and Biological Engineering*, 12, 17-25.
- Khleifat, K.M., Tarawneh, K.A., Ali Wedyan, M., Al-Tarawneh, A.A., Al-Sharafa, K., 2008. Growth kinetics and toxicity of *Enterobacter cloacae* grown on linear alkylbenzene sulfonate as sole carbon source. *Current Microbiology*, 57(4): 364-370. <https://doi.org/10.1007/s00284-008-9203-z>
- Klaus, T., Joerger, R., Olsson, E., Granqvist, C.-G., 1999. Silver-based crystalline nanoparticles, microbially fabricated. *Proceedings of the National Academy of Sciences*, 96(24): 13611-13614. <https://doi.org/10.1073/pnas.96.24.13611>
- Lee, S.H. and Jun, B.-H., 2019. Silver nanoparticles: synthesis and application for nanomedicine. *International Journal of Molecular Sciences*, 20(4): 865. <https://doi.org/10.3390/ijms20040865>

- Otoni, C.A., Simes, M.F., Fernandes, S., Dos Santos, J.G., Da Silva, E.S., de Souza, R.F.B., Maiorano, A.E., 2017. Screening of filamentous fungi for antimicrobial silver nanoparticles synthesis. *AMB Express*, 7(1): 1-10.
<https://doi.org/10.1186/s13568-017-0332-2>
- Qaralleh, H., Khleifat, K.M., Al-Limoun, M.O., Alzedaneen, F.Y., Al-Tawarah, N., 2019. Antibacterial and synergistic effect of biosynthesized silver nanoparticles using the fungi *Tritirachium oryzae* W5H with essential oil of *Centaurea damascena* to enhance conventional antibiotics activity. *Advances in Natural Sciences: Nanoscience and Nanotechnology*, 10(2): 025016.
<https://doi.org/10.1088/2043-6254/ab2867>
- Rahimi, G., Alizadeh, F., Khodavandi, A., 2016. Mycosynthesis of silver nanoparticles from *Candida albicans* and its antibacterial activity against *Escherichia coli* and *Staphylococcus aureus*. *Tropical Journal of Pharmaceutical Research*, 15(2): 371-375.
<https://doi.org/10.4314/tjpr.v15i2.21>
- Riaz, A., Khan, S.U.-D., Zeeshan, A., Khan, S.U., Hassan, M., Muhammad, T., 2021. Thermal analysis of peristaltic flow of nanosized particles within a curved channel with second-order partial slip and porous medium. *Journal of Thermal Analysis and Calorimetry*, 143(3): 1997-2009.
<https://doi.org/10.1007/s10973-020-09454-9>
- Sastry, M., Ahmad, A., Khan, M.I., Kumar, R., 2003. Biosynthesis of metal nanoparticles using fungi and actinomycete. *Current Science*, 162-170.
- Satalkar, P., Elger, B.S., Shaw, D.M., 2016. Defining nano, nanotechnology and nanomedicine: why should it matter? *Science and Engineering Ethics*, 22(5): 1255-1276.
<https://doi.org/10.1007/s11948-015-9705-6>
- Sergeev, G.B. and Shabatina, T.I., 2008. Cryochemistry of nanometals. *Colloids and Surfaces A: Physicochemical and Engineering Aspects*, 313, 18-22.
<https://doi.org/10.1016/j.colsurfa.2007.04.064>
- Singh, R., Wagh, P., Wadhvani, S., Gaidhani, S., Kumbhar, A., Bellare, J., Chopade, B.A., 2013. Synthesis, optimization, and characterization of silver nanoparticles from *Acinetobacter calcoaceticus* and their enhanced antibacterial activity when combined with antibiotics. *International Journal of Nanomedicine*, 8, 4277.
<https://doi.org/10.2147/IJN.S48913>
- Sondi, I. and Salopek-Sondi, B., 2004. Silver nanoparticles as antimicrobial agent: a case study on *E. coli* as a model for Gram-negative bacteria. *Journal of Colloid and Interface Science*, 275(1): 177-182.
<https://doi.org/10.1016/j.jcis.2004.02.012>
- Sosa, I.O., Noguez, C., Barrera, R.G., 2003. Optical properties of metal nanoparticles with arbitrary shapes. *The Journal of Physical Chemistry B*, 107(26): 6269-6275.
<https://doi.org/10.1021/jp0274076>
- Tarawneh, K.A., AlTawarah, N.M., AbdelGhani, A.H., AlMajali, A.M., Khleifat, K.M., 2009. Characterization of verotoxigenic *Escherichia coli* (VTEC) isolates from faeces of small ruminants and environmental samples in Southern Jordan. *Journal of Basic Microbiology*, 49(3): 310-317.
<https://doi.org/10.1002/jobm.200800060>
- Tarawneh, O., Alwahsh, W., Abul-Futouh, H., Al-Samad, L.A., Hamadneh, L., Abu Mahfouz, H., Fadhil Abed, A., 2021. Determination of Antimicrobial and Antibiofilm Activity of Combined LVX and AMP Impregnated in p (HEMA) Hydrogel. *Applied Sciences*, 11(18): 8345.
<https://doi.org/10.3390/app11188345>
- Xu, Z.P., Zeng, Q.H., Lu, G.Q., Yu, A.B., 2006. Inorganic nanoparticles as carriers for efficient cellular delivery. *Chemical Engineering Science*, 61(3): 1027-1040.
<https://doi.org/10.1016/j.ces.2005.06.019>
- Yousef, I., Oran, S., Alqaraleh, M., Bustanji, M., 2021. Evaluation of cytotoxic, antioxidant and antibacterial activities of *Origanum dayi*, *Salvia palaestina* and *Bongardia chrysogonum* plants growing wild in Jordan. *Tropical Journal of Natural Product Research*, 5(1): 66-70.
<https://doi.org/10.26538/tjnpr/v5i1.7>